https://doi.org/10.2352/CIC.2025.33.1.3

LUT-based Skin Spectrum Estimation System

Fangjia Du, Minchen Wei*; The Hong Kong Polytechnic University; *minchen.wei@polyu.edu.hk

Abstract

The measurement of diffuse skin reflectance spectrum has important applications, but require accurate and fast measurements. In this study, we proposed several methods for reconstructing the diffuse skin reflectance spectrum using several existing datasets. These methods can reconstruct the spectrum of an area by only capturing the images under several LED illuminations, instead of using comprehensive systems. A comprehensive system is being built to collect a ground-truth dataset, and also used to test the performance of the proposed methods.

Introduction

The reflectance spectrum of skin contains important information. Great efforts have been made to investigate how to measure or reconstruct the skin spectrum. For example, Wang et al. [1] used a spectroradiometer to measure the spectrum reflected from skin under a fluorescent lighting, and also that reflected from a reflectance standard. Hyperspectral cameras were used in [2, 3, 4] to capture the hyperspectral images of human skin. These measurements typically take tens of seconds, which is time consuming and also introduces errors due to the unavoidable movement. In contrast, efforts have also been made to reconstruct the spectrum using the images captured by cameras, which can be achieved through a mapping from low to high dimensions [5, 6] or using neural networks [7, 8]. Some of these work considered the specular and diffuse reflections by placing polarizers to only capture the diffuse reflection.

The reflection of skin is also of great interest in the computer graphics community, as they care about the optical properties, in terms of reflectance factor and directional properties, for rendering. Debevec et al. [9] developed a light stage system to measure the Bidirectional Reflectance Distribution Function (BRDF) of human face, which helps to characterize the reflectance factor at an arbitrary combination of the illumination and camera directions. Polarizers were placed in front of the light sources and cameras to remove the specular reflection. Ghosh et al. [10] further modified the system and proposed algorithms that iteratively isolate the diffuse reflection from the specular reflection. Due to the storage constraints, they are not able to quickly capture high-precision diffuse reflection information, in terms of the spectral reflectance distribution.

In this study, we propose a system to rapidly capture the image of skin under several LED illumination, which can then be used to reconstruct the spectral reflectance distribution using a look-up-table (LUT) derived based on the biophysical model of skin.

Method

Construction of a dataset using skin model and derivation of the RDF

The Kubelka-Munk (K-M) model characterizes photon propagation in multi-layer media through a two-flux approximation, employing a simplified system of differential equations to characterize scattering, absorption, and interlayer interactions [11, 12]. The model requires various biological parameters, including melanin and hemoglobin volume fractions, as the inputs. Based on several prior works (i.e., [13, 14]), we generated a dataset comprising 20790 spectral reflectance distributions of skin from 400 to 700 nm with an interval of 1 nm by varying the parameters of the K-M model. Figure 1 shows the spectral reflectance distributions of the 20790 skin samples.

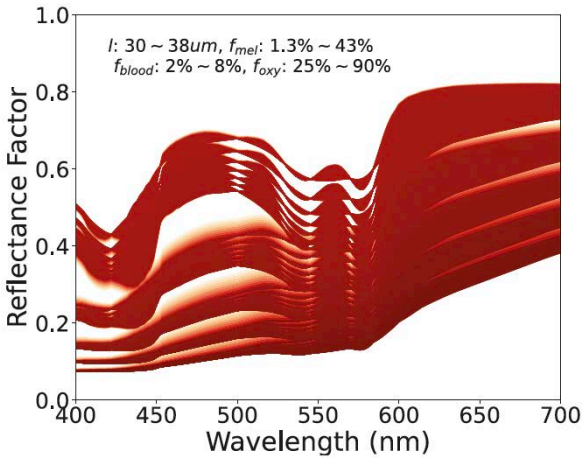

Figure 1. Spectral reflectance distributions of 20790 skin samples constructed using the K-M model.

The camera response of an illuminated sample can be expressed as:

$$P_i = \int_{\lambda} E(\lambda)R(\lambda)\mathbb{S}_i(\lambda)d\lambda, i = R, G, B \tag{1}$$

where $\mathbb{S}_i(\lambda)$ is the spectral sensitivity function of the camera RGB channels, $E(\lambda)$ is the spectral power distribution of the illumination, and $R(\lambda)$ is the spectral reflectance distribution of the illuminated surface. This can also be transformed into a matrix format, with n discrete wavelengths:

$$P_s = dR_s^T diag(E_s)\mathbb{S} \tag{2}$$

where P_s is the R, G, B channel response of the camera, R_s is a vector for the spectral reflectance distribution, E_s is a vector of the

spectral power distribution, and $\mathbb{S}$ is a n by 3 matrix representing the camera sensitivity functions of the three channels. With this, the responses of m samples captured under l illuminations can be expressed as:

$$\begin{aligned}\mathcal{R} &= R\Theta\Phi \\ &= R\left[diag(\mathbb{S}_R), \quad diag(\mathbb{S}_G), \quad diag(\mathbb{S}_B)\right]\begin{bmatrix} E & & \\ & E & \\ & & E \end{bmatrix}\end{aligned} \tag{3}$$

where Θ and Φ are the spectral sensitivity functions of the camera and the spectral power distribution of the illuminations, $\mathbb{S}_R, \mathbb{S}_B, \mathbb{S}_B$ are the column vectors of the camera spectral sensitivity functions $\mathbb{S}$ in R, G, B channel respectively. $\mathcal{R}$ is a m by $3l$ matrix, with each row for responses of the camera R channel of one sample under all the illumination, followed by the G and B channel responses. We define the matrix $\mathcal{R}$ as the ***R**esponse **D**istribution **F**unction(RDF)* with variables $R, E, \mathbb{S}$:

$$\mathcal{R} = \mathcal{R}(E, R, \mathbb{S}) \tag{4}$$

Then, for a collection of samples R_{tr} captured under a series of illumination with the spectral power distribution E_ρ using a camera with the spectral sensitivity function $\mathbb{S}_\rho$, we can derive the RDF of the samples through:

$$\mathcal{R}_{tr} = R_{tr}\Theta_\rho\Phi_\rho, \qquad \mathcal{R}_{te} = \sigma \odot R_{te}\Theta_\rho\Phi_\rho \tag{5}$$

where $\odot$ is the Hadamard product and σ is a $3l$-element scaling vector which can be derived using a reflectance standard:

$$\begin{aligned}&\sigma_i = \text{mean}(\mathcal{R}_{w,v,i} \oslash \mathcal{R}_{w,c,i}), \;\; \mathcal{R}'_{te,i} = \frac{\mathcal{R}_{te,i}}{\sigma_i} \\ &\quad i = R, G, B\end{aligned} \tag{6}$$

where $\mathcal{R}_{w,c}$ is theoretical reflectance standard response and $\mathcal{R}_{w,v}$ is the RDF of the reflectance standard, $\oslash$ represents the element-wise division. To remove the cross-talk effect, the calculations are performed on each of the three channels individually, which can then be used to scale the RDF of the samples through:

$$\mathcal{R}'_{te} = \left[\mathcal{R}'_{te,R}, \mathcal{R}'_{te,G}, \mathcal{R}'_{te,B}\right] \tag{7}$$

Proposed method of reconstruction of skin spectral reflectance

Here, we propose three methods for reconstructing the spectral reflectance distribution of a test skin sample based on the image captured by a camera.

Direct Searching Method. The most straightforward method is through a direct search (DS), looking for the RDF value of the samples in the dataset that is the most similar to the RDF of the test sample. In particular, multiple illumination is needed to reduce the possibility of metamerism. Here, we use the root mean square error (RMSE) to calculate the similarity, with a smaller RMSE value for a higher similarity.

$$T = \text{argmin}(RMSE(\mathcal{R}'_{te}, \mathcal{R}_{tr})) \tag{8}$$

where T is the index of the sample in the dataset whose RDF is the most similar to the test sample RDF. With the identified RDF, the spectrum can be reconstructed:

$$R_{pr} = R_{te}(T) \tag{9}$$

2-Step Scale Unit Vector. Though the dataset constructed using the K-M model covers a wide range of conditions by varying the parameters, it is still possible that some skin spectral reflectance distributions are missing due to the setting of the parameter interval and the accuracy of the model itself. To address such a possible weakness, we propose a two-step scale unit vector (2-StepUV) method. Firstly, we identify the RDF of the sample in the dataset that has the most similar shape as the RDF of the test sample, without considering the magnitude, and then derive the scaling factor to scale the spectral reflectance distribution of the identified sample. The identification of the sample in the dataset that has the most similar shape can be performed by normalizing the RDF of the test sample and the RDFs of all the samples in the dataset:

$$\mathcal{R}_{tr,u} = \frac{\mathcal{R}_{tr}}{\|\mathcal{R}_{tr}\|}, \;\; \mathcal{R}'_{te,u} = \frac{\mathcal{R}'_{te}}{\left\|\mathcal{R}'_{te}\right\|} \tag{10}$$

where $\mathcal{R}_{tr,u}$ and $\mathcal{R}'_{te,u}$ represent the unit RDF of the test sample and those of all the samples in the dataset respectively. Then the most similar unit RDF can be identified through the calculation of the angular error using:

$$T_u = \text{argmin}(RMSE(\mathcal{R}'_{te,u}, \mathcal{R}_{tr,u})) \tag{11}$$

where T_u is the index of the sample in the dataset whose unit RDF has the smallest angular error to the unit RDF of the test sample. A factor can then be calculated to scale the identified RDF to derive the reconstructed spectrum of the test sample:

$$R_{pr} = \text{mean}(\mathcal{R}'_{te} \oslash \mathcal{R}_{tr,T_u})R_{tr}(T_u) \tag{12}$$

Weighting Table. The two above methods try to find the spectral reflectance distribution in the dataset that is the most similar to the test sample in terms of amplitude and shape, which significantly depends on the range of the samples included in the dataset. We propose a Weighting Table method to the RDF in the dataset and synthesize the reconstructed spectrum of the test sample. We start from the RDF of the samples $\mathcal{R}_{tr}$ in the dataset and the scaled RDF of the test sample $\mathcal{R}'_{te}$, and the weighting table method can be used to reconstruct the spectrum of the test sample:

$$R_{pr} = WR_{tr} = \begin{bmatrix} w_1 & w_2 & \cdots & w_n \end{bmatrix}\begin{bmatrix} R_{tr,1} \\ R_{tr,2} \\ \vdots \\ R_{tr,n} \end{bmatrix} \tag{13}$$

where W is the weighting table, which is a n dimension vector with each element w being the weighting factor for each sample in the dataset. And the weighting factor can be calculated by:

$$w'_i = \frac{1}{RMSE(\mathcal{R}'_{te,i}, \mathcal{R}_{tr,i}) + \delta}, \quad i = 1, 2, \ldots, n \tag{14}$$

with

$$w_i = \frac{w'_i}{\sum_{i=1}^{n} w'_i} \tag{15}$$

The weighting factors are calculated from the RMSE value between the scaled RDF of the test sample and the RDFs of the samples in the dataset. A small value δ (i.e., $1e-3$) is used to prevent the denominator from being zero. Equation 15 is used to rescale the weighting factor to ensure that the sum of the weighting factors is less than one.

Experiment

We developed a system to test the proposed methods and also to collect spectral reflectance distributions of skin samples.

System

We developed a lighting system to illuminate a skin area, which included two lighting units. Each unit contained 10 LED channels, with the peak wavelengths of 450 ~ 455nm, 465 ~ 480nm, 490 ~ 495nm, 520 ~ 530nm, 530 ~ 540nm, 560 ~ 570nm, 590 ~ 595nm, 605 ~ 615nm, 620 ~ 630nm and 650 ~ 660nm. In order to create a relative uniform illumination on the skin, a diffuser was placed in front of the LED array. In addition, a polarizer was placed in front of the diffuser, which was used to remove the specular reflection together with the polarizer in front of the camera. A FLIR BLACKFLY S chromatic camera was used to capture the images, which uses a Sony IMX183 sensor and has a resolution of 5472×3648 and a frame rate up to 18FPS. The spectral sensitivity function of the camera was measured in our laboratory using a monochromator and a spectroradiometer. The exposure time of the camera was set to different values for capturing the skin area and the reflectance standard, with the exposure time and camera response validated to have a linear relationship.

Figure 2 shows the setup of the system, with the two lighting units illuminating the surface from the direction of 45 degree and the camera and the spectroradiometer placed to capture the surface perpendicularly. As mentioned above, the polarizors were placed in front of the lighting units and the camera/spectroradiometer to remove the specular reflection.

The skin area was illuminated by the 10 LED channels sequentially, with the camera capturing an image under each illumination. After that, all the 10 channels were switched on together to produce a white illumination on the skin area. The spectroradiometer was then used to measure the spectrum reflected from a smaller area of the skin. Figure 3 shows the experiment procedure. Capturing the images under the 10 LED illumination can be achieved within 10 seconds.

In addition to capturing and measuring the skin area, we also performed the same capturing and measurement on a reflectance standard, with the data used for data analyses.

Results and Discussions

Figure 4 shows the images captured by the camera for the skin area (i.e., an area on an Asian person's wrist region) and the reflectance standard. It is obviously that the images of the skin are darker than those of the reflectance standard. And the details of the blood vessels can be observed when the skin was illuminated under a red illumination. The red dot is the small area where the spectral

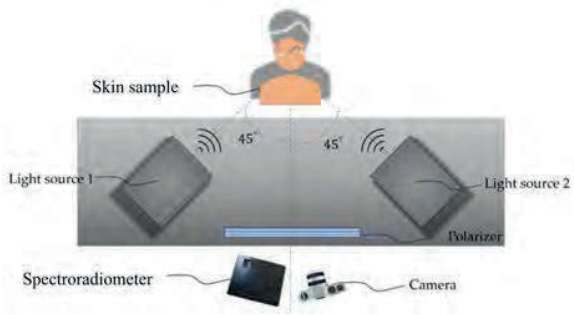

Figure 2. Illustration of the system built by us.

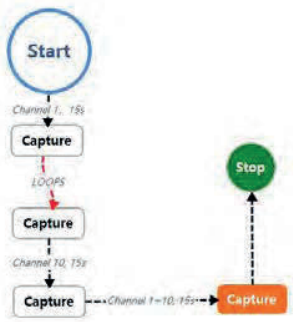

Figure 3. Flow chart of the experiment procedure.

measurements were performed, which was also used as the skin sample in the following analyses. With the pixel values extracted from the skin images and the reflectance standard images at that point, the errors caused by any non-uniformity can be completed avoided. With the reflected spectra from the skin E_{smp} and the reflectance standard measured under the white illumination, the ground-truth of the skin spectral reflectance distribution can be calculated as:

$$R_{GT} = E_{smp} \oslash E \otimes R_w \tag{16}$$

where R_{GT} is the ground-truth spectral reflectance distribution of the skin sample, E is the spectral power distribution of the illumination, and R_w is the spectral reflectance of the reflectance standard, which was 0.99 according to the calibration certificate, $\oslash$ and $\otimes$ are element-wise division and multiplication respectively.

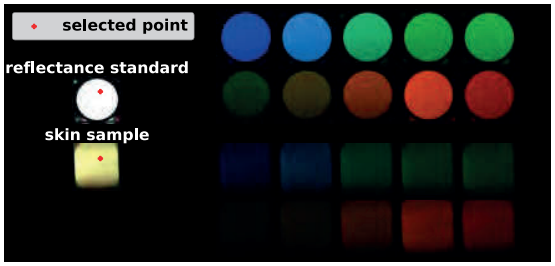

Figure 4. Images of the reflectance standard and skin area under the different illumination captured by the camera in the experiment, with the red dot showing the pixels (i.e., sample) used in the analyses.

With the captured images of the skin sample and the reflectance standard, the scalers of each channel can be calculated, which was then used to map the RDF of the skin sample. Figure 4 shows the RDF of the skin sample and also the RDFs derived from the constructed dataset. It is obvious that the RDF of the skin sample is within the range of the RDFs of the dataset, suggesting that the dataset is likely to include such a sample.

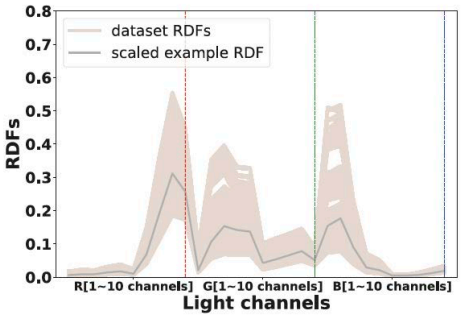

Figure 5. RDF of the skin sample collected in the experiment, and the RDFs of the samples included in the constructed dataset

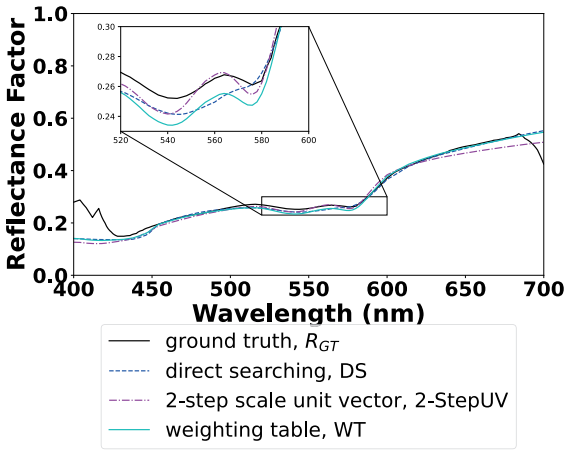

Figure 6. Reconstructed spectral reflectance distribution of the skin sample labelled in Figure 4 using the three proposed methods and its ground-truth, with a close-up of the wavelength region between 520 and 600 nm

Discussion

The RDF of the skin sample was then used to reconstruct the spectral reflectance distribution using the three proposed methods. Figure 6 shows the reconstructed and the ground-truth spectral reflectance distributions.

For the ground-truth spectral reflectance distribution, the higher and lower values at the short and long wavelengths were likely caused by the noises, since the 10 LED channels produce little radiation at these wavelengths.

For the three proposed methods, the overall shape of the reconstructed spectral reflectance distributions were very similar to the ground-truth. The 2-StepUV method produced lower values between 650 ~ 700 nm, but it can produce the most similar 'W' shape and magnitude between 520 and 600 nm, which is the most critical wavelength region for the spectral reflectance distribution of skin. In contrast, the weighting table method can produce a similar shape, but the amplitude is a little lower. To numerically characterize the performance of the three methods, we calculated the RMSE and Goodness-of-Fit Coefficient (GFC) and the CIELAB and MLAB [15] color difference using the reconstructed and ground-truth spectral reflectance distributions, with Table 1 summarizing the values of these characterizations.

GFC characterizes the similarity between two vectors:

$$GFC = \frac{\hat{R}^T R}{\left\|\hat{R}^T \hat{R}\right\| \left\|R^T R\right\|} \tag{17}$$

where $\hat{R}$ is the reconstructed spectral reflectance distribution and R is the ground-truth spectral reflectance distribution. The MLAB colour space is proposed by DU et al. [15], which is a modified version of the CIELAB colour space for better characterize the perceived color difference. It can be observed that the three methods all had good performance, especially in terms of the color differences. Among the three methods, the DS method was found to have slightly better performance. It is worthwhile to point out that the calculations were performed using the ground-truth spectral reflectance distribution shown in Figure 6, which is believed to have discrepancies at the two ends, so the actual performance of these methods should be better. This also suggests the necessity to collect more accurate ground-truth spectral reflectance distribution.

Table 1 Summary of values characterizing the performance of the three proposed methods.

Method	RMSE	GFC%	ΔE_{ab}	ΔE_{Mab}
DS	**0.0346**	**99.48**	2.21	**1.28**
2-StepUV	0.0387	99.42	2.88	1.69
WT	0.0353	99.47	**1.99**	1.41

We then picked five locations on the skin area, as shown in Figure 7, and used the proposed DS method to reconstruct the spectral reflectance distributions. It can be observed that the reconstructed spectra were very similar, in terms of the magnitude, with the estimated melanin concentration being similar. There is also a variation between 500 and 600 nm, which is caused by the estimated blood and hemoglobin concentration.

With the results of a single point and five points, we further expanded the analyses to an area of 320×380 pixels, as shown in Figure 8. The selected area is in the center of the captured skin area. All the reconstructed spectral reflectance distributions share a similar shape, but different magnitudes. This was likely due to the non-uniform reflection caused by the non-flat skin surface, suggesting the importance of the skin texture [2]. It took around 2.8 ms to reconstruct one spectral reflectance distribution using a PC with 12GEN @Intel 20 cores 2.10 GHz CPU and 32GB RAM,

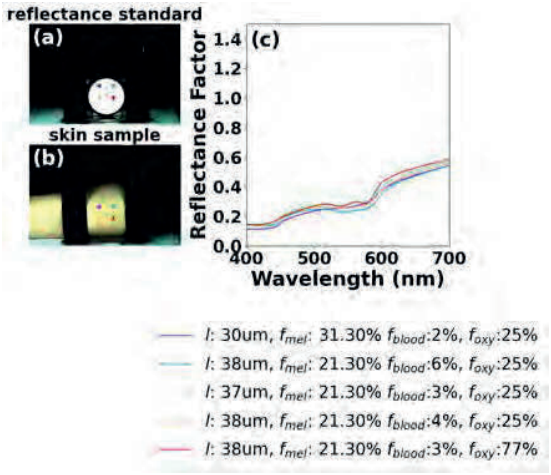

Figure 7. Results of the reconstruction on five skin samples using the DS method. (a) Selected samples on the reflectance standard; (b) selected samples on the skin area; (c) reconstructed spectral reflectance distributions with the estimated skin characteristics.

with a total of around 6 minutes to reconstruct all the pixels in the selected region.

All the results and analyses suggest the effectiveness of using the proposed method to reconstruct the spectral reflectance distributions of skin based on the images captured under several LED illumination. We are making efforts to identify the optimal LEDs for reduce the time of capturing and further improve the accuracy, and also to measure the ground-truth spectral reflectance distribution with a higher accuracy.

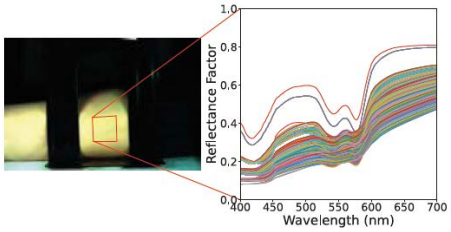

Figure 8. Results of the reconstruction of a region using the DS method.

Conclusion

In this paper, we constructed a dataset of skin spectral reflectance distribution. We developed a system using 10-channel LED devices and cameras to capture images of skin area, and proposed three methods to reconstruct the spectral reflectance distribution using the captured images. The results suggest the effectiveness of the proposed methods, which can be used for a single location or an area. The results also suggested the necessity to further investigate the optimal LED channels to improve the performance of the reconstruction and how to measure the ground-truth of skin spectral reflectance distribution with a higher accuracy.

Reference

[1] Yuzhao Wang et al. “Spectrophotometric measurement of human skin colour”. *Color Research & Application* 42.6 (2017), pp. 764–774.

[2] Lou Gevaux et al. “Three-dimensional maps of human skin properties on full face with shadows using 3-D hyperspectral imaging”. *Journal of Biomedical Optics* 24.6 (2019), pp. 066002–066002.

[3] Pierre Seroul et al. “Model-based skin pigment cartography by high-resolution hyperspectral imaging”. *Journal of Electronic Imaging* 69.6 (2016), pp. 48–56.

[4] Christian Fischer and Ioanna Kakoulli. “Multispectral and hyperspectral imaging technologies in conservation: current research and potential applications”. *Studies in Conservation* 51.sup1 (2006), pp. 3–16.

[5] Bin Cao, Ningfang Liao, and Haobo Cheng. “Spectral reflectance reconstruction from RGB images based on weighting smaller color difference group”. *Color Research & Application* 42.3 (2017), pp. 327–332.

[6] Morteza Maali Amiri and Mark D Fairchild. “A strategy toward spectral and colorimetric color reproduction using ordinary digital cameras”. *Color Research & Application* 43.5 (2018), pp. 675–684.

[7] Romuald Jolivot, Yannick Benezeth, and Franck Marzani. “Skin parameter map retrieval from a dedicated multispectral imaging system applied to dermatology/cosmetology”. *Journal of Biomedical Imaging* (2013), pp. 26–26.

[8] Yuliya Gitlina et al. “Practical measurement and reconstruction of spectral skin reflectance”. *Computer graphics forum*. Vol. 39. 4. 2020, pp. 75–89.

[9] Paul Debevec et al. “Acquiring the reflectance field of a human face”. *Proceedings of the 27th Annual Conference on Computer Graphics and Interactive Techniques*. 2000, pp. 145–156.

[10] Abhijeet Ghosh et al. “Multiview face capture using polarized spherical gradient illumination”. *Proceedings of the 2011 SIGGRAPH Asia Conference*. 2011, pp. 1–10.

[11] Paul Kubelka. “Ein beitrag zur optik der farbanstriche”. *Z. tech. Phys* 12 (1931), pp. 593–601.

[12] Mathieu Hébert, Roger D Hersch, and Patrick Emmel. “Fundamentals of optics and radiometry for color reproduction”. *Handbook of Digital Imaging* (2015), pp. 1–57.

[13] Aravind Krishnaswamy and Gladimir VG Baranoski. “A biophysically-based spectral model of light interaction with human skin”. *Computer Graphics Forum*. Vol. 23. 3. Wiley Online Library. 2004, pp. 331–340.

[14] Carlos Aliaga, Christophe Hery, and Mengqi Xia. “Estimation of spectral biophysical skin properties from captured RGB albedo”. *arXiv preprint arXiv:2201.10695* (2022).

[15] Fangjia Du, Yang Xu, and Changjun Li. “Modified CIELAB Uniform Color Space”. *Acta Optica Sinica* 42.1 (2022), p. 0133001.

Author Biography

Fangjia Du is a PhD student at The Hong Kong Polytechnic University. His research mainly focus on skin color and shape reconstruction.

Minchen Wei is a professor at The Hong Kong Polytechnic University. His research mainly focus on color science and imaging science.